International Journal of Nanoelectronics and Materials

In Press, Accepted Manuscript – Note to user

Improved the sensitivity and limit of detection of surface alloying SERS sensors by controlling mixing ratio of trimetallic (Ag-Au-Pd) nanoparticles

Russul M. Shehab [1*] , Alwan M. Alwan [2]

[1]Department of Radiology and Sonar Techniques, Al-Esraa University College, Baghdad, Iraq.
[2]Department of Applied Sciences, University of Technology, Baghdad-Iraq

Received 21 April 2022, Revised 31 July 2022, Accepted 25 August 2022

ABSTRACT

In this study, three different types of hybrid structures SERS sensors made from different mixing ratio of trimetallic (Ag-Au-Pd) nanoparticles of [Au1: Ag1: Pd1] , [Au1: Ag2: Pd1] , [Au1: Ag2: Pd2] in surface alloying forms deposited on macro porous silicon (macroPsi) layer were created and extensively tested. By using a simple and fast immersion process, trimetallic (Ag-Au-Pd) nanoparticles were created utilizing ion reduction of numerous metallic salts on a macro porous silicon (macroPsi) layer. The macroPsi layers were created using a laser assisted etching (LAE) technique for 15 minutes with a constant density of approximately (28mA/c.m2). At a constant concentration (10-3 M) of HAu.Cl4, Ag.NO3 and Pd.Cl2 to synthesize Au-NPs, Ag-NPs and Pd-NPs, immersion processes with various mixing ratios were performed. The hybrid structures of SERS sensors were examined using XRD, FE-SEM, and Raman microscopes. The sensors were tested at different concentrations from 10-6 to10-12 of MB target molecules. The SERS trimetallic sensors demonstrated a considerable reliance on hot spot zones among trimetallic nanoparticles. Higher enhancement factor with lower detection limit of Raman signal was obtained from (Au 1: Ag 2: Pd 2) hybrid structures SERS sensor of about 1.5×1010 and 10-14 respectively, due to extra ordinary specific surface area and high surface density forming trimetallic nanoparticles . The variations of mixing ratio of trimetallic (Ag-Au-Pd) provide an effective pathway to develop the sensors performance towards detection of lower concentrations.

Keywords: Ion reduction process, P-Si SERS sensors, Trimetallic Au-Ag-Pd alloy-nanoparticles.

1. INTRODUCTION

The metallic nanoparticles NPs are showing strong dipolar excitation as localized. Surface .plasmon .resonances (L.S.P.R), where the mobility of the free electron cloud which is confined at the metal-dielectric interface will be set in resonance through optical radiation at specific wave-length based on the types and the dimensions of nanoparticles [1]. It has been indicated that such resonance oscillation is one of the metal's distinctive characteristic that is presently utilized in a lot of applications such as nano-photonics, bio-markers, photonic crystals, in addition to bio-sensing [2–9]. LSPR frequencies regarding metallic NPs are very dependent on surrounding medium, shape, size, as well as morphology. Some other metals such as Ni, Pd, and Pt showed excellent plasmonics response [`10-14], even though that the noble metals (Cu, Ag, and Au) are dominating the scientific studies because of their distinctive optical properties [15–17]. The colloidal solution regarding metal NPs showing excellent absorption in visible region as well as showing extremely intense color, whereas the other metals showing weak and broadband in UV region [18-20]. Due to the fairly easy surface chemistry, the potential to attach molecules, stability, and bio-compatibility, coinage metals have been of high importance in some applications, such as biosensors and drug- delivery [21,22].

*E-mail: Russul.Mohammed@esraa.edu.iq

Copper (Cu), gold (Au), and spherical silver (Ag) NPs have L.S.P.R absorption band in red, green, and blue regions, respectively that might be subjected to tuning through different shapes and sizes [23-25].

Surface enhanced Raman scattering (SERS) is integrating rise sensitivity-levels with the spectroscopic accuracy. Therefore, huge capability with regard to the chemical and bio molecular sensing [1–4]. The LSPR excitation in gold and silver NPs is showing strong extinction as well as scattering spectra which are recently were utilized for significant SERS improvement. With regard to the SERS signals, typically extremely weak impact, was indicated to be improved through order of 1013 with the existence of nano-meter-sized Ag "hot particles", that allow the potential to investigate Raman scattering at sole molecular scale [5,6]. The significance regarding extensive applications of Raman spectroscopy with the use of roughened metallic surfaces is developing re-producible and improving the practical substrates with regard to analytical targets, i.e., for high sensitivity in detecting trace contaminants and pollutants. Basically, trimetallic Au–Ag–Pd nanoparticle catalysis outperformed bimetallic catalysts and monometallic. Significant catalytic activity of trimetallic nanoparticles could be related to consecutive electrical effect among elements in particle [7]. The control of the metallic nanoparticles like surface morphology, density, particle size, shape and elemental structure of alloy NPs have specified as major aspects for tuning the device's sensitivity and chemical reactivity. [8]. In this work, three different types of surface alloying hybrid structures SERS sensors made from different mixing ratio of trimetallic (Ag-Au-Pd) nanoparticles have been reported. The main aim is to enhance the performance of the sensor by increasing enhancement factor with lowering limit of detection of Raman signal through controlling the hot spot regions among the trimetallic nanoparticles.

2. MATERIAL AND METHODS

2.1 Chemical Materials

Methylene blue MB powder (C16H18N3SCl) with a purity of 95% purchased from FLUKA was used to prepare concentrations ranging from 10-6 to 10-12 of MB. To present suitable 40 percent hydrofluoric acid (HIMEDIA) and etching solution (20 percent HF), diluted with high purity ethanol (99.8 percent). Ag-NO3, Pd-Cl2, HAu-Cl4:3H2O salts were obtained from Sigma–Aldrich Germany, and the purity of the salts was approximately (99.99%), (99.9%), and (99.8%), respectively, and were utilized to generate the needed electrolyte solution for the ion reduction process. To prepare an aqueous solution, a 1 mM Pd-Cl2 salt was dissolved in 0.15 M HF and a few drops of 37 percent HCL at 60 °C under magnetic stirring for around thirty minutes. Making an aqueous solution with a concentration of 1 mM, the Ag-NO3 salt was dissolved in triply distilled water. Using distilled-water and 2.9M HF, prepare HAuCl4•3H2O at a concentration of (1 mM). These salt solutions' and MB's concentrations were calculated according to the following formula (1) [14]:

$$\text{Molarity} = \frac{\frac{W}{M.Wt}}{V} \quad (1)$$

M.Wt (g/Mol) represents the molecular weight , V represents the size of the dissolved solution and W (g) represents the weight of the salts.

2.2 Preparation of Hybrid Structures Trimetallic SERS Sensor

To prepare n-type Si 100 substrate with an electrical resistivity of 10cm and macro.PSi substrate were employed. Si native oxide was eliminated from Si substrate prior to etching operation by immersing the substrates for 4 minutes in a 12 percent HF-aqueous solution. In an etching mixture solution of 40 percent HF and 99.999 percent C2H5OH in a ratio of 1:1, as-prepared macroPSi layers were created using LAE. The Si substrate was etched for fifteen min with a constant density of approximately (28mA/c.m2). with power density of about 25 mW/cm2. and 630 nm laser irradiation. After the etching process, the as-prepared macroPSi substrate was washed in liquid and dried in the open air.

Macro Psi was modified by trimetallic nanoparticles by usage of an immersion process of porous layer in aqueous solution of 10-3 M HAu-Cl4, 10-3 M Ag-NO3, 10-3 M Pd-Cl2 with different mixing ratio of [Au1: Ag1: Pd1] , [Au1: Ag2: Pd1] , [Au1: Ag2: Pd2] to prepare three different types of hybrid structures SERS sensors S1 , S2 and S3 respectively. The following cathodic reactions occur during the ion reduction of Au, Ag, and Pd, respectively. [15-18]:

$$2Si + 6HF \longrightarrow H_2SiF_6 + 4H^+ + 4e \quad (2)$$

$$Au^{3+} + 3e^- \longrightarrow Au \quad (3)$$

$$Ag^+ + e^- \longrightarrow Ag \quad (4)$$

$$Pd^{2+} + 2e^- \longrightarrow Pd \quad (5)$$

Figure 1 shows a proposed schematic depiction of the preparation for trimetallic surface alloy structures. (1). Force interaction between ion of the metals and substrate macroPsi will also play a significant role in changing tri-layer deposition.

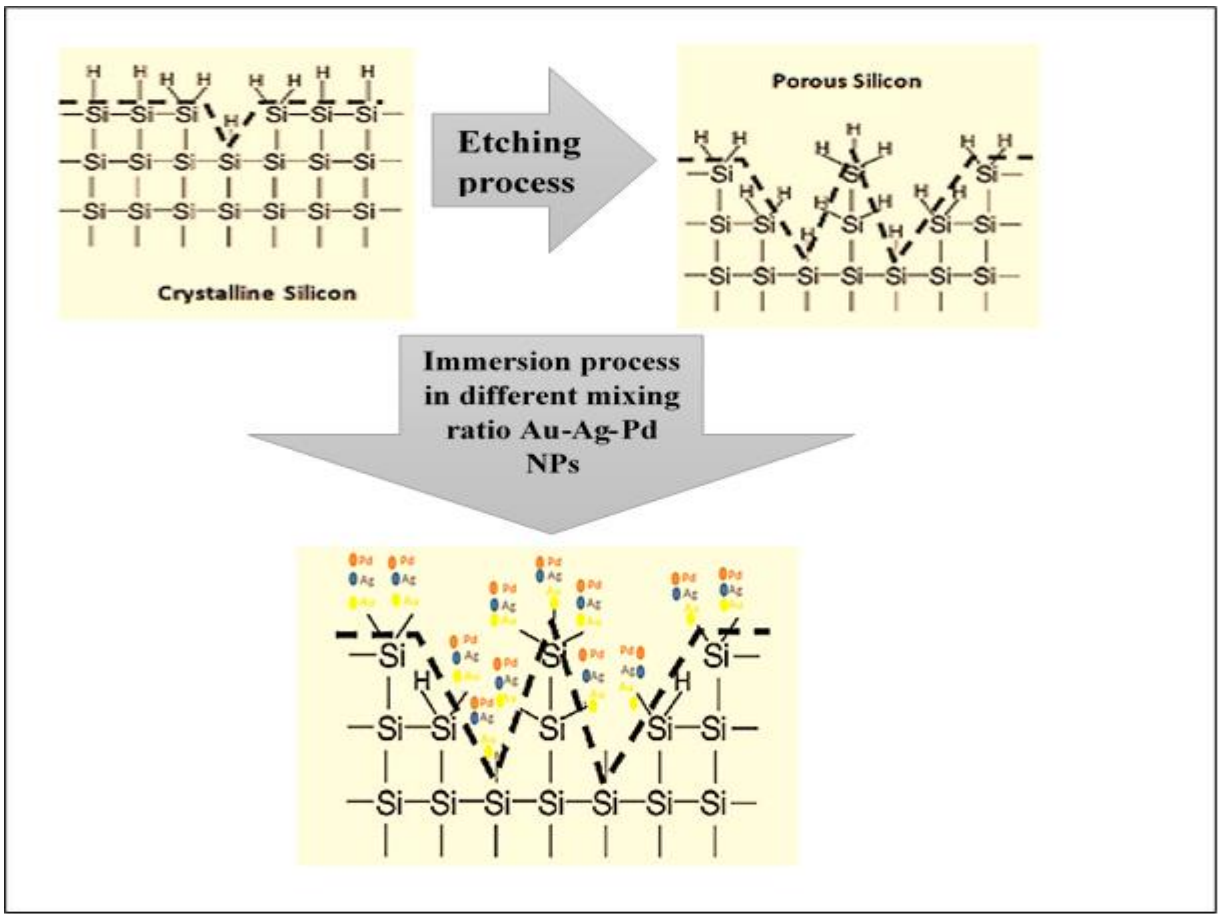

Figure 1 . Schematic illustration of preparation surface alloying hybrid structures SERS sensor with trimetallic Ag-Au-Pd NPs/macro Psi based on the Volmer–Weber growth model.

3. RESULTS AND DISCUSSION

3.1 Structural Characterization

Pore size distribution and image of FE-SEM of the as-prepared macroPSi layer are shown in Figures 2(a,b). The surface is clearly made up of dense homogeneous semi-spherical pores. Pore size is around 0.5 to 6.5 m, with the top of the pore size distribution being about (0.5) m and standard deviation(σ) is 78.949. PSi acts as a minimizing agent in the ion reduction. thus, clearly minimize metallic ions having positive reduction possibility with regard to hydrogen [26- 28].

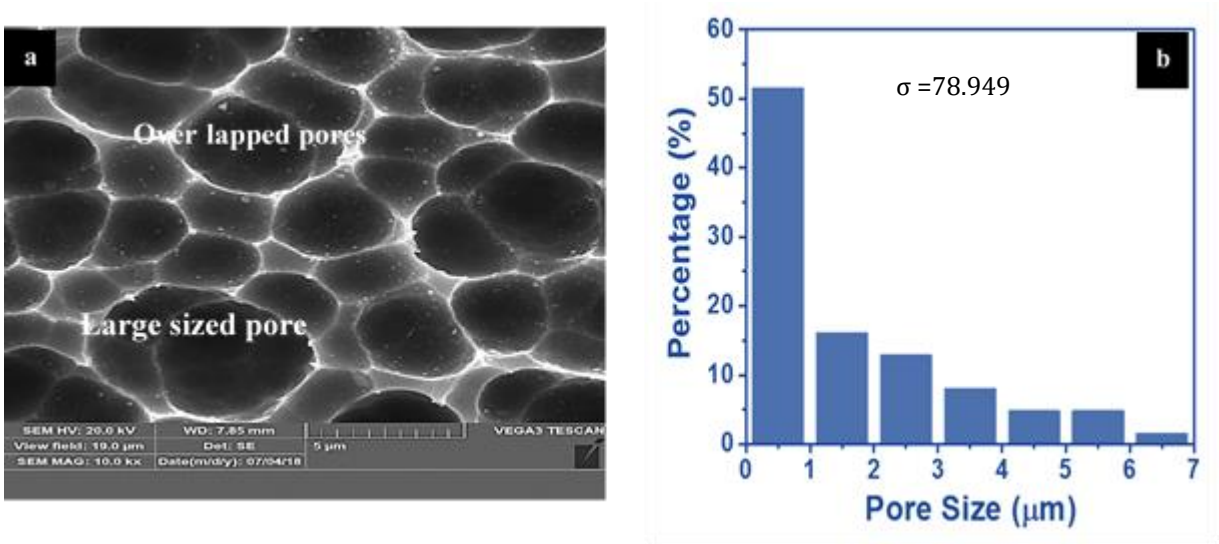

Figure 2. (a) FE-SEM of as-prepared macro PSi (b) Statistical distribution of pore sizes.

Figure (3) depicts typical FE-SEM images of three different types of hybrid structures SERS sensors S1, S2 and S3. Figure (3a) show FE-SEM images of Au-Ag-Pd NPs/macroPSi at mix ratio (Au1: Ag 1: Pd 1) were deposited on the macroPSi surface are primarily found in pore walls, particularly when their combined size exceeds the pore volume. Electron affinity of metallic ions, Pd, Ag and Au were around (0.562, 1.304, and 2.308) eV, the major cause of the creation of the surface alloying process. [18]. The surface morphology of all types of trimetallic nanoparticles sensors, is consisted of large density of tiny particles ranging in size from (8) to (17) nm, with the major volume being around (13) nm, as shown in the figure (3a) S1 sensor . While, figure (3b) at mix ratio(Au 1: Ag 2: Pd 2) S2 sensor, it's shown The aggregation of Au-Ag-Pd NPs on the Si surface has a greater chances of formed nanoparticles is larger than that of S1 sensor. The size distribution of formed NPs of S2 sensor, with a major value of around (9) nm and a range of (6) to (13) nm (figure 3b) and the surface density of trimetallic nanoparticles is lower than that of the others sensors. The histogram of hot spot regions size distribution among trimetallic nanoparticles is illustrated in figure 4a-c. As shown in S2 sensor , a small size , high density of surface alloys trimetallic nanoparticles. In comparison to the other S1 and S2 sensors, sensor S2 exhibits a high level of spatial homogeneity of Au-Ag-Pd NPs over the macroPSi surface. The histogram of hot spot sizes among the formed nanoparticles is spanning from (15) to (40) nm, and the size distribution's peak is about (20) nm, with a percentage of (38%) and standard deviation(σ) is 4.918 as can be seen in the figure (4a) S1 sensor. While, figure (4b) at mix ratio (Au 1: Ag 2: Pd 2) S2 sensor, it's shown that the hot spot sizes is varied from 10 to 35 nanometers, with a maximum peak of 20 nanometers with percent (46 %) and σ is 3.344 (Figure 4b). Finally for S3 sensor fig4c, The volume fraction of trimetallic nanoparticles around (25-45) nm, peak of around (30) nm with percent (33 %) and σ is 6.188.

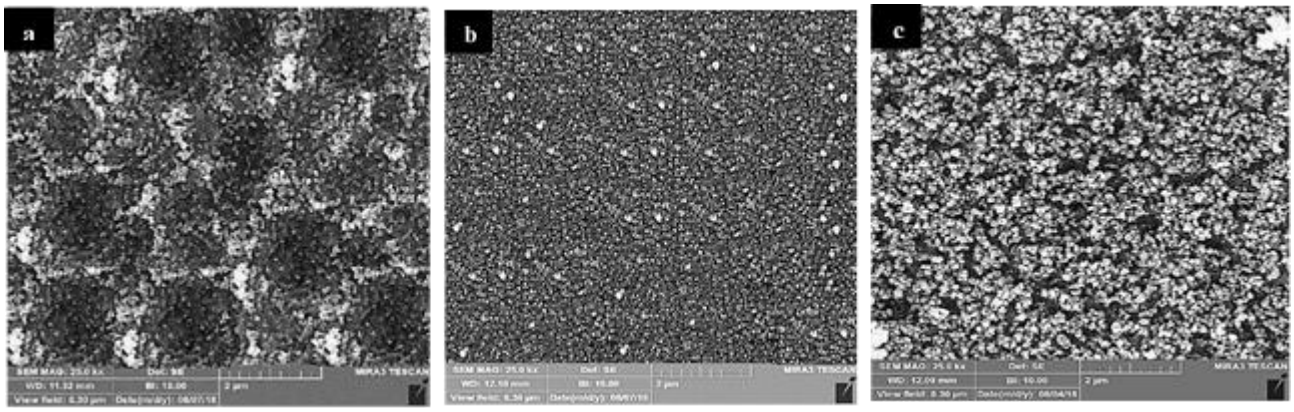

Figure 3. FE-SEM images of modified as-formed macroPsi layers of (a) S1, (b) S2, (c) S3 sensors.

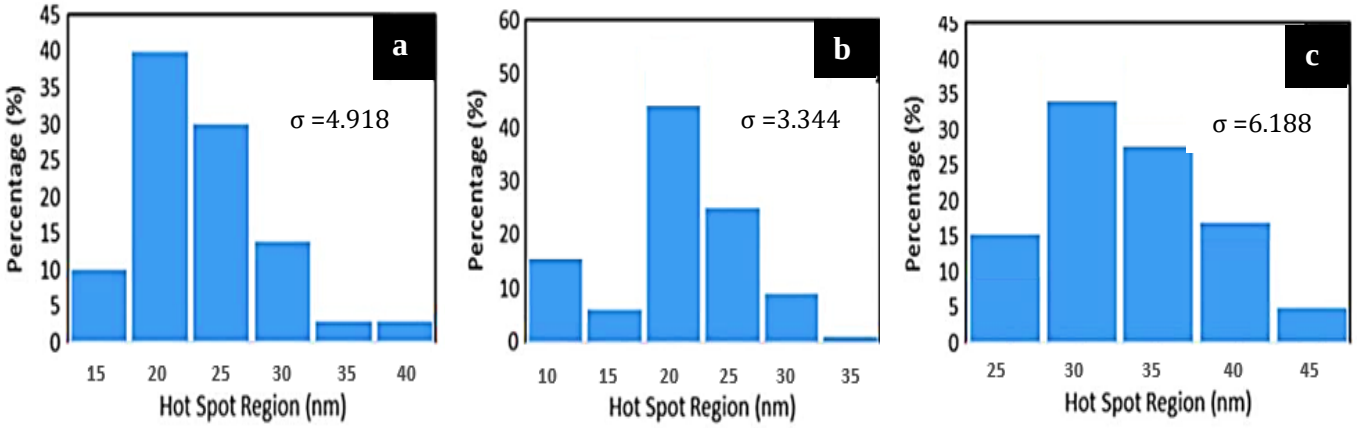

Figure 4. Histogram of hot spot regions size distribution of modified as-formed macroPsi layers of (a) S1, (b) S2, (c) S3 sensors.

The structural properties related to the Au–Ag–PdNPs deposited over Si surface were studied through analyzing its XRD pattern. Figure.5 (a-c), illustrates the diffraction peak structure for Au-Ag-Pd/macroPsi surface alloying nano structure. The lattice characteristics of Au-Ag-Pd alloy nanoparticles are identical, (4.065, 4.079 and 3.859). There seems to be an interaction between the peaks for Ao ,gold, silver, and palladium, accordingly, indicating that these metals are alloyed nanoparticles. [23, 24]. The nanoparticles volume of NPs was calculated by the Sherrers equation (6) [25].

$$L = \frac{K\lambda}{B\cos\theta} \qquad (6)$$

The specific surface area is indeed one of the eligible criteria for nanostructured materials, and given by equation (7) [26]:

$$S.S.A. = \frac{6000}{D * \rho} \qquad (7)$$

Where, ρ is the densities of Pd, Ag, and Au are 12.023, 10.5, and 19.3g/cm3, correspondingly, whereas the densities of trimetallic are around 12.1758, 13.09789, 16.4041, and 12.13426 g/cm3, respectively. These numbers can be figured out with the help of equation (8) [27]:

$$D = \frac{a*\rho + b*\rho + c*\rho}{a+b+c} \quad (8)$$

Where, a = wt. % Au, c = wt. % Pd, D = density of trimetallic Au-Ag-Pd nanoparticles (g/cm3), and b = wt. % Ag and. From the obtained data of Au-Ag-Pd/macroPsi surface alloying nano structure, its clear that the S2 sensore has lower nanoprticle sizes of about 5nm and hence higher S.S.A of about 102(m2/gm) . this is strongly related with the availibilty of ions in reduction so;ution , so the lower formed nanopoarticles sizes is achieved with high density of ions i.e high rate of generation nanoparticles .

Table 1. Nanoparticle size and S.S.A of S_1, S_2 and S_3

Sensors' Types	Mixing Ratio	Phase(111)	
		Nanoparticle size(nm)	S.S.A(m^2/g_m)
S_1	$Au_1:Ag_1:Pd_1$	11	45
S_2	$Au_1:Ag_2:Pd_1$	17.65	21.5
S_3	$Au_1:Ag_2:Pd_2$	5	102

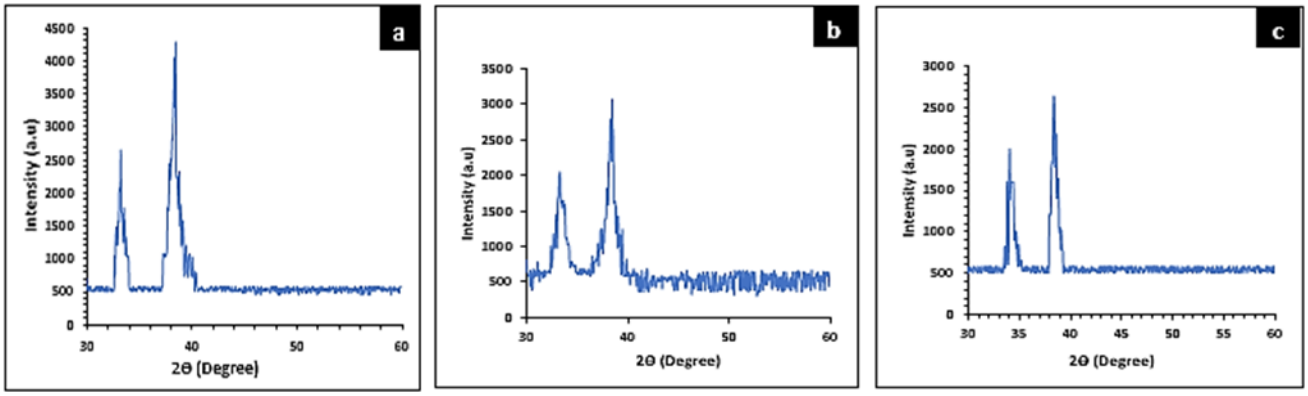

Figure 5. XRD Pattern of S.S.A of (a) S1, (b) S2 and (c) S3 Sensors

3.2 Raman spectra of trimetallic NPs surface alloying SERS sensors

Three different type of surface alloying SERS sensors S1, S2 and S3 were fabricated and tested extensively against different concentrations of Methylene blue (MB) target molecule. In the surface alloying SERS sensors, the macroPsi substrate was evaluated at 10-4 M after being dipped in MB at concentrations of 10−6, 10−8,10−10 and 10−12 M. See Figure 6, The (MB) Raman spectrum for macroSi (without the trimetallic nanoparticles) exhibits a very modest Raman signal with a distinct peak at 1625 cm-1 (main peak). Figure 7 describes SERS spectra of surface alloying SERS sensors S1, S2 and S3. The Raman bonds have seven distinct peaks that can be found in the varying of 400-1600 cm−1, at 1625, 1396, 1302, 1154 and 772 ,502, 448 cm−1. Those peaks are inextricably linked to C–C, C-N, C–H, C-S-C and C-N-C bond stretching vibrations. The Raman enhancement effect of raman spectra is given by the following formula (9) [30]. Table 2 illustrates the enhancement factor IF as a function to sensors types.

$$IF = \frac{I_{SERS} / C_{SERS}}{I_{RS}/C_{RS}} \quad (9)$$

Where IRS is the Raman signal of the Si with a concentration of CRS and ISERS is SERS signal peak intensity at a specific level concentration of CSERS With regard to this study, the highest SERS IF has been indicated to be 1.5×1010 when mixing ratio of Au-Ag-Pd NPs/macroPSi hetero structures is (Au 1: Ag 2: Pd 2) S2 sensor. The limit of detection (LOD) for MB has been computed via the equation (10):

$$LOD = 3Sd/\ d \quad (10)$$

The SERS peak intensity standard deviation of the calculated outcome at Raman shift is denoted by Sd, and the calibrated curve slope is denoted by d.

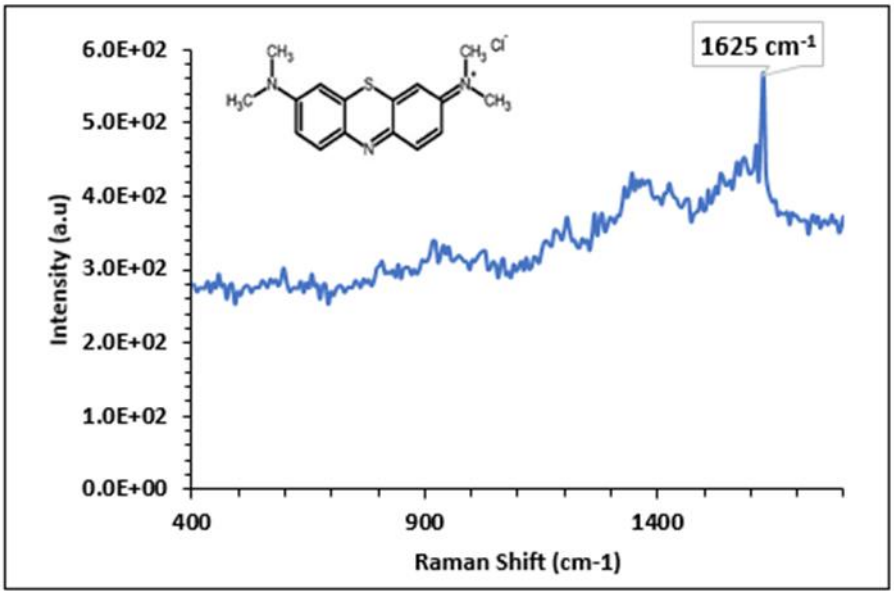

Figure 6. Chemical structure and Raman spectrum of MB of as-prepared macroSi with 10-4M concentration.

To establish a quantitative analyzing of the surface alloying SERS sensors S1, S2 and S3, a relation among the measured peak intensity 1625 cm−1 (main peak) is seen in Figure 8. This figure shows a linear the connection among them at concentration of 10-6 to 10-12 M. Correlation offers ultra-high Raman signals. The chief explanation for this performance is due to the density of hot spots among trimetallic alloys. In extra, the S.S.A of the of trimetallic NPs surface alloying nanoparticles themselves.

An effective energy transition among the trimetallic NPs and molecules of MB intimate the locations with a lot of hot spots can increase the sensitivity and limit of detection of surface alloying SERS sensors towards the target molecules and therefore; boosts Raman signal. The effective significant variable for evaluating the action of the fabricated sensors, IF be figured out with the help of equation 9. Figure (8) shows the IF against the concentrations of MB solution. Imposing a continuous increase in the IF with a reduction in the concentration of the target molecule. Very small molecule concentrations increase the likelihood of locating the target molecule, resulting in its recognition and an IF increase due to SERS signal strengthening.

The limit of detection of Raman signal LOD of tri metallic surface alloying SERS nanoparticles / macroPSi layer sensors for MB was computed via using equation (10). The limit of detection of about

(10-13, 10-14 and 0.5* 10-12 and M) were attained with S1, S2 and S3 respectively. The obtained LOD limit of S2 trimetallic sensor is substantially lower than what had previously been reported in mono and bimetallic SERS sensors [26, 28, 29]

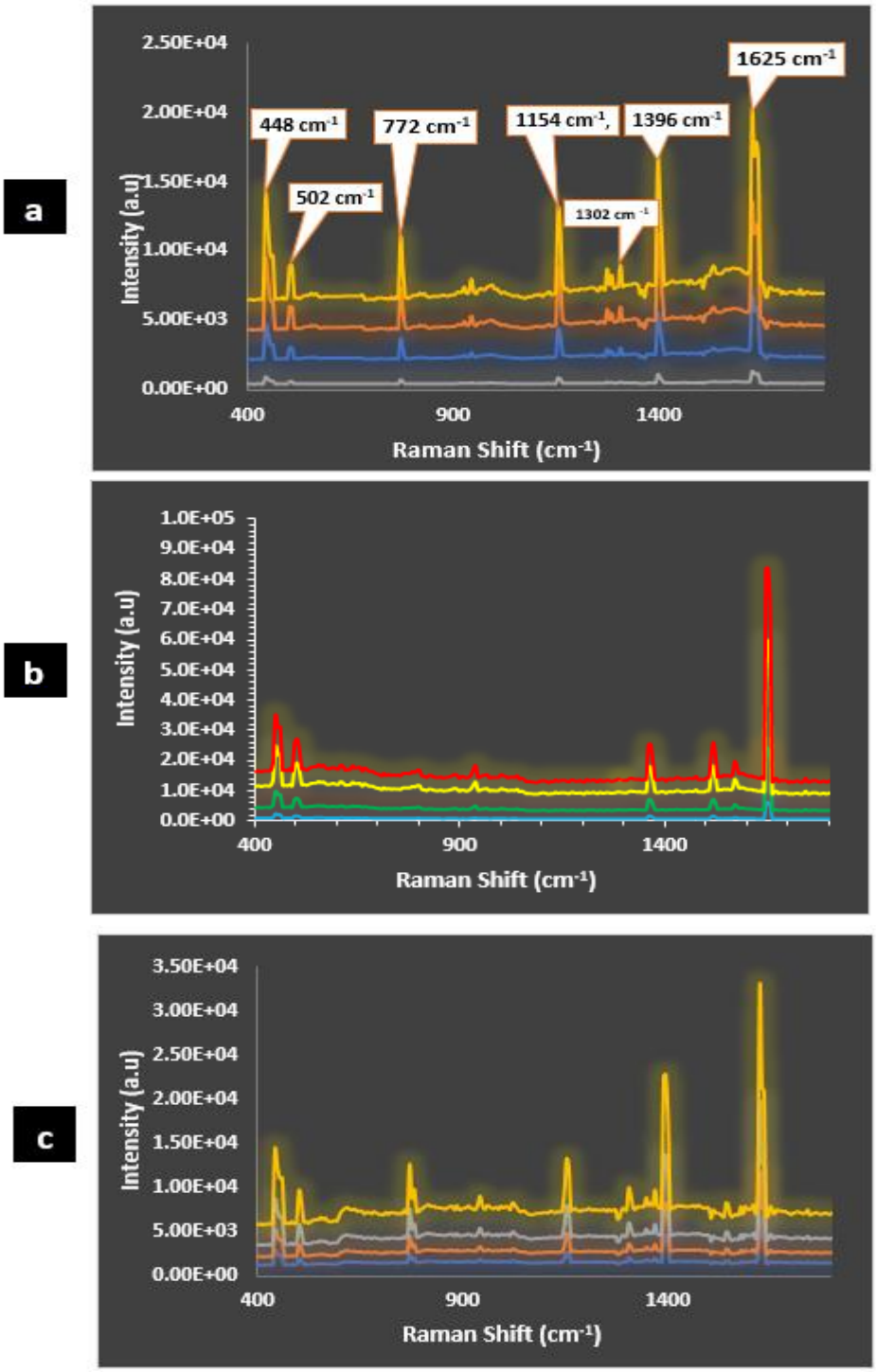

Figure 7. SERS spectra of surface alloying SERS sensors S1, S2 and S3 at concentrations 10^{-6}, 10^{-8}, 10^{-10} and 10^{-12}M.

Table 2. The values of surface alloying SERS sensors

MB concentration (M)	Enhancement Factor (EF) S1 sensor	Enhancement Factor (EF) S2 sensor	Enhancement Factor (EF) S3 sensor
10^{-6}	2.4×10^{2}	1.1×10^{3}	1.2×10^{3}
10^{-8}	1.2×10^{5}	4.2×10^{5}	3.5×10^{5}
10^{-10}	2.4×10^{7}	1.1×10^{8}	3.5×10^{7}
10^{-12}	3.5×10^{9}	1.5×10^{10}	5.8×10^{9}

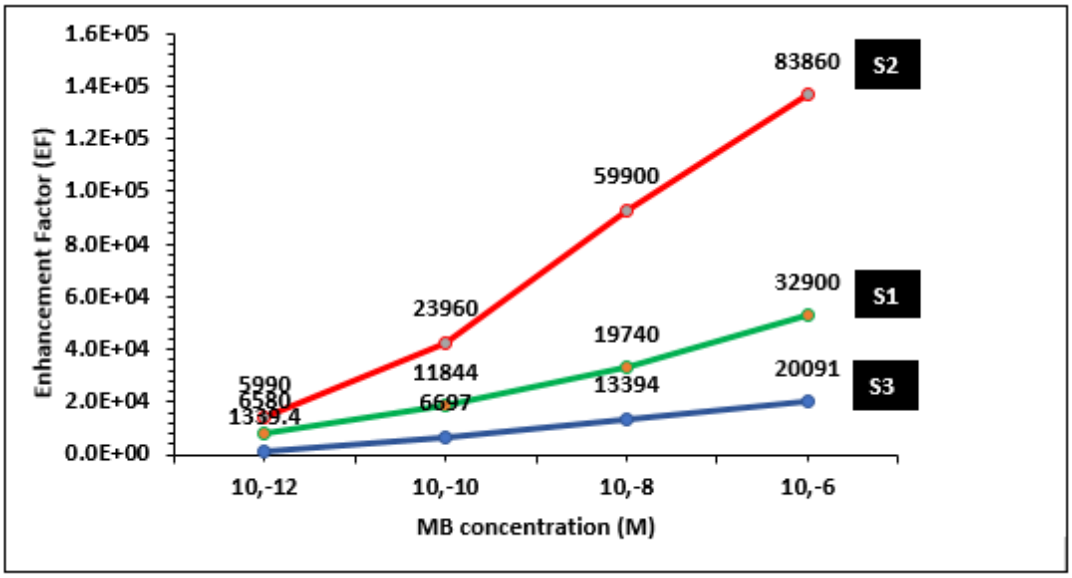

Figure 8. Relationship between MB concentrations and the enhancement factor of S1, S2 and S3 for the main peak 1625 cm^{-1}.

4. CONCLUSION

In this paper, an efficient improvement of the sensitivity and limit of detection SERS sensors was carried out by controlling mixing ratio of trimetallic (Ag-Au-Pd) nanoparticles for the discovery procedure of very minimum concentration of MB target-molecules. An easy and low-cost ion decrease procedure was utilized to create three types of Ag-Au-PdNPs/ macro P-Si SERS sensors. Updating mixing ratio of trimetallic (Ag-Au-Pd) ions guide to the formation of low-dimensional structures that are efficient and essentially uniformly distributed Ag-Au-Pd NPs hotspot regions nanoparticles with a high specific surface area. The plasmonics characteristics of trimetallic (Ag-Au-Pd) nanoparticles were employed for sensing the ultra-minimum 10-12 M concentration of MB molecules. Higher IF with minimum limit of detection of Raman signal was achieved from (Au 1: Ag 2: Pd 2) hybrid structures SERS sensor of about 1.5×1010 and 10-14 respectively. The

variations of mixing ratio of trimetallic (Ag-Au-Pd) provide an effective pathway to develop the sensors performance towards detection of lower concentrations.

ACKNOWLEDGEMENTS

The authors are beholden to the Applied Sciences Department -University of Technology and Al-Esraa University College for their cooperation.

REFERENCES

[1] Petryayeva, Eleonora, and Ulrich J. Krull. "Localized surface plasmon resonance: Nanostructures, bioassays and biosensing—A review." Analytica chimica acta 706, no. 1 (2011): 8-24.
[2] Zhao, Qianying, Ruiqi Duan, Jialing Yuan, Yi Quan, Huan Yang, and Mingrong Xi. "A reusable localized surface plasmon resonance biosensor for quantitative detection of serum squamous cell carcinoma antigen in cervical cancer patients based on silver nanoparticles array." International Journal of Nanomedicine 9 (2014): 1097.
[3] Alwan, M. A., Mohammed, S. M., & Russul M. Shehab (2020). Optimizing plasmonic characteristics of Ag-AuNPs/Nanohillocks Si Heterostructures for efficient SERS performance.
[4] Hong, Yoochan, Minhee Ku, Eugene Lee, Jin-Suck Suh, Yong-Min Huh, Dae-Sung Yoon, and Jaemoon Yang. "Localized surface plasmon resonance based nanobiosensor for biomarker detection of invasive cancer cells." Journal of biomedical optics 19, no. 5 (2013): 051202.
[5] Zhang, Xinping, Shengfei Feng, Jian Zhang, Tianrui Zhai, Hongmei Liu, and Zhaoguang Pang. "Sensors based on plasmonic-photonic coupling in metallic photonic crystals." Sensors 12, no. 9 (2012): 12082-12097.
[6] Zhou, Cheng. "Localized surface plasmonic resonance study of silver nanocubes for photonic crystal fiber sensor." Optics and Lasers in Engineering 50, no. 11 (2012): 1592-1595.
[7] Zayats, Anatoly V., Igor I. Smolyaninov, and Alexei A. Maradudin. "Nano-optics of surface plasmon polaritons." Physics reports 408, no. 3-4 (2005): 131-314.
[8] Zeng, Shuwen, Dominique Baillargeat, Ho-Pui Ho, and Ken-Tye Yong. "Nanomaterials enhanced surface plasmon resonance for biological and chemical sensing applications." Chemical Society Reviews 43, no. 10 (2014): 3426-3452.
[9] Frederix, Filip, Jean-Michel Friedt, Kang-Hoon Choi, Wim Laureyn, Andrew Campitelli, Dirk Mondelaers, Guido Maes, and Gustaaf Borghs. "Biosensing based on light absorption of nanoscaled gold and silver particles." Analytical Chemistry 75, no. 24 (2003): 6894-6900.
[10] Miller, Molly M., and Anne A. Lazarides. "Sensitivity of metal nanoparticle surface plasmon resonance to the dielectric environment." The Journal of Physical Chemistry B 109, no. 46 (2005): 21556-21565.
[11] Nuzzo, R. G. "Nanostructured plasmonic sensors." Chem. Rev 108 (2008): 494-521.
[12] Chen, Huanjun, Xiaoshan Kou, Zhi Yang, Weihai Ni, and Jianfang Wang. "Shape-and size-dependent refractive index sensitivity of gold nanoparticles." Langmuir 24, no. 10 (2008): 5233-5237.
[13] Zijlstra, Peter, Pedro MR Paulo, and Michel Orrit. "Optical detection of single non-absorbing molecules using the surface plasmon resonance of a gold nanorod." Nature nanotechnology 7, no. 6 (2012): 379.
[14] Katyal, Jyoti, and R. K. Soni. "Size-and shape-dependent plasmonic properties of aluminum nanoparticles for nanosensing applications." Journal of Modern Optics 60, no. 20 (2013): 1717-1728.
[15] Langhammer, Christoph, Zhe Yuan, Igor Zorić, and Bengt Kasemo. "Plasmonic properties of supported Pt and Pd nanostructures." Nano letters 6, no. 4 (2006): 833-838.
[16] Zoric, Igor, Michael Zach, Bengt Kasemo, and Christoph Langhammer. "Gold, platinum, and aluminum nanodisk plasmons: material independence, subradiance, and damping mechanisms." ACS nano 5, no. 4 (2011): 2535-2546.
[17] Pirzadeh, Zhaleh, Tavakol Pakizeh, Vladimir Miljkovic, Christoph Langhammer, and Alexandre Dmitriev. "Plasmon–interband coupling in nickel nanoantennas." Acs Photonics 1, no. 3 (2014): 158-162.
[18] Cobley, Claire M., Sara E. Skrabalak, Dean J. Campbell, and Younan Xia. "Shape-controlled synthesis of silver nanoparticles for plasmonic and sensing applications." Plasmonics 4, no. 2 (2009): 171-179.

[19] Lee, Kyeong-Seok, and Mostafa A. El-Sayed. "Gold and silver nanoparticles in sensing and imaging: sensitivity of plasmon response to size, shape, and metal composition." The Journal of Physical Chemistry B 110, no. 39 (2006): 19220-19225.

[20] Chan, George H., Jing Zhao, Erin M. Hicks, George C. Schatz, and Richard P.Van Duyne. "Plasmonic properties of copper nanoparticles fabricated by nanosphere lithography." Nano Letters 7, no. 7 (2007): 1947-1952.

[21] Park, Hyejin, Hiroshi Tsutsumi, and Hisakazu Mihara. "Cell penetration and cell-selective drug delivery using α-helix peptides conjugated with gold nanoparticles." Biomaterials 34, no. 20 (2013): 4872-4879.

[22] Shi, Weihong, Justin Casas, Meenakshi Venkataramasubramani, and Liang Tang. "Synthesis and characterization of gold nanoparticles with plasmon absorbance wavelength tunable from visible to near infrared region." ISRN Nanomaterials 2012 (2012).

[23] Liu, Sha, Guanying Chen, Paras N. Prasad, and Mark T. Swihart. "Synthesis of monodisperse Au, Ag, and Au–Ag alloy nanoparticles with tunable size and surface plasmon resonance frequency." Chemistry of Materials 23, no. 18 (2011): 4098-4101.

[24] Noguez, Cecilia. "Surface plasmons on metal nanoparticles: the influence of shape and physical environment." The Journal of Physical Chemistry C 111, no. 10 (2007): 3806-3819.25. Lee, Kuang-Che, Su-Jien Lin, Chih-Hong Lin, Chih-Song Tsai, and Yu-Jen Lu. "Size effect of Ag nanoparticles on surface plasmon resonance." Surface and Coatings Technology 202, no. 22-23 (2008): 5339-5342.

[25] Alwan, A. M., Russul M. Shehab (2015). Characterization of (Nanostructures Silver/Silicon Nano Porous) Active Substrates for Surface Enhanced Raman Scattering (SERS) as a Function to Porous Silicon Parameters. Engineering and Technology Journal, 33(3 Part (B) Scientific).

[26] Wali, Layla A., Alwan M. Alwan, Amer B. Dheyab, and Duaa A. Hashim. "Excellent fabrication of Pd-Ag NPs/PSi photocatalyst based on bimetallic nanoparticles for improving methylene blue photocatalytic degradation." Optik 179 (2019): 708-717.

[27] Alwan, A. M., Russul M. Shehab. (2015). Preparation and Characterization of Nano Porous Silicon for Chemical Detection Applications. Engineering and Technology Journal, 33(2 Part (B) Scientific).

[28] Alwan, Alwan M; Mohammed, Mohammed S; Russul M. Shehab. "Optimization of an ultra-sensitive Ag core-Au shell nanoparticle/Si Surface-enhanced Raman scattering (SERS) sensor." AIP Conference Proceedings. Vol. 2307. No. 1. AIP Publishing LLC, 2020.

[29] Alwan, A. M., Mohammed, M. S., & Russul M. Shehab (2021). Modified laser-etched silicon covered with bimetallic Ag–Au Alloy nanoparticles for high-performance SERS: laser wavelength dependence. Indian Journal of Physics, 95(9), 1843-1851.

[30] Alwan, A. M., Mohammed, M. S., & Russul M. Shehab (2020). The Performance of Plasmonic Gold and Silver Nanoparticle-Based SERS Sensors. Iraqi Journal of Science, 1320-1327.